Eur. Phys. J. B **45**, 261–266 (2005)
DOI: 10.1140/epjb/e2005-00074-x

THE EUROPEAN PHYSICAL JOURNAL B

Magnetization and polarized neutron reflectivity experiments on patterned exchange bias structures

K. Temst[1,a], E. Girgis[1,b], R.D. Portugal[1,c], H. Loosvelt[1], E. Popova[1], M.J. Van Bael[1], C. Van Haesendonck[1], H. Fritzsche[2,d], M. Gierlings[2], L.H.A. Leunissen[3], and R. Jonckheere[3]

[1] Laboratorium voor Vaste-Stoffysica en Magnetisme, K.U. Leuven, Celestijnenlaan 200 D, 3001 Leuven, Belgium
[2] Hahn-Meitner-Institut, BENSC, Glienicker Strasse 100, 14109 Berlin, Germany
[3] IMEC vzw, Kapeldreef 75, 3001 Leuven, Belgium

Received 15 September 2004
Published online 15 March 2005 –

Abstract. Patterned Co/CoO thin film structures have been investigated by magnetization and polarized neutron reflectivity measurements in order to study the influence of finite size and shape anisotropy effects on the magnetization reversal. An anomaly was found in the upper branch of the hysteresis loops, probably caused by incomplete bias in the patterned structures. The asymmetry in magnetization reversal mechanism commonly found in the two branches of the hysteresis loops of unpatterned Co/CoO layers is altered in the patterned structures, consistent with the existence of interfacial domains.

PACS. 75.70.Cn Magnetic properties of interfaces – 75.25.+z Spin arrangements in magnetically ordered materials

1 Introduction

The steady advance in lithography and deposition techniques has created opportunities for the production of well-defined micron and nanometer sized magnetic structures. From a scientific point of view, the motivation is twofold: first, new physical effects are encountered when the mesoscopic regime is explored in which the size of the magnetic structures becomes of the same order of magnitude as some relevant physical length scale [1,2] or when the magnetic entities interact with each other [3], with a semiconducting layer [4], or with a superconducting layer [5,6]. The second main reason is that the better understanding of the physics governing these mesoscopic structures can be used in large-scale industrial applications like, e.g., magnetic storage media, computer memories, and sensors. The latter is certainly the case for patterned exchange bias structures. Although exchange bias materials are already commonly used in certain devices, the precise mechanism of the exchange bias effect has not yet been elucidated [7,8] and there is currently ample attention for the influence of finite size and artificially imposed anisotropy effects on exchange bias [9–16].

In this paper we discuss magnetization measurements carried out with a superconducting quantum interference device (SQUID) and with a vibrating sample magnetometer (VSM), as well as polarized neutron reflectivity (PNR) experiments. Our aim is to study the effects of finite dimensions and shape anisotropy on the exchange bias behavior of patterned Co/CoO structures. PNR has the particular and unique advantage of providing a magnetic depth profile and direct information about the magnetization reversal mechanism [17,18]. This is a very attractive feature for the study of particular exchange bias systems, such as Fe/FeF_2 and Co/CoO where it has been observed that the magnetization reversal mechanism can be different in the descending and the ascending branches of the hysteresis loop [19–22]. Two types of patterns will be discussed: small squares (with a side between 200 nm and 900 nm and set in a square grid with period varying between 1000 nm and 1700 nm, respectively) and wires with a very high aspect ratio (width of 2 μm and length of 2 cm). The lateral period of the wires is 15 μm.

2 Experimental details

The samples were prepared by a combination of lithography methods and deposition techniques. A resist mask was made on oxidized Si wafers, after which the deposition of the magnetic material occurred. A lift-off step in boiling acetone removes the resist. For the small squares electron beam lithography was used. An area of 5 mm by 5 mm

[a] e-mail: kristiaan.temst@fys.kuleuven.ac.be
[b] *Permanent address*: National Research Center, Egypt
[c] *Present address*: Dept. of Physics, University of Missouri-Columbia, USA
[d] *Present address*: National Research Council, Canada

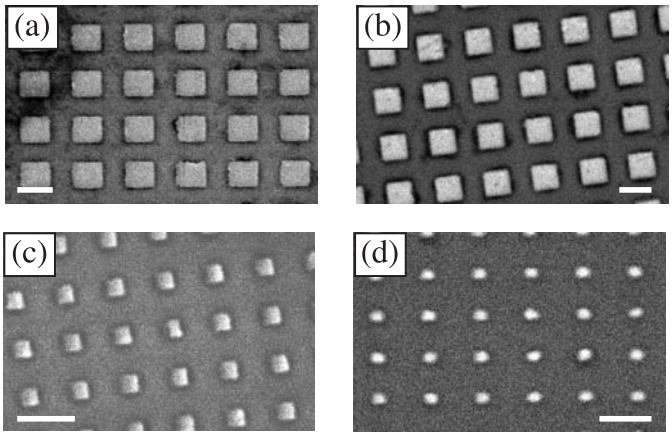

Fig. 1. SEM pictures of the square Co/CoO structures. The white marker corresponds to a length of 1 μm. The side of the squares is (a) 900 nm, (b) 800 nm, (c) 400 nm, and (d) 200 nm and the center-to-center distances are 1700 nm, 1600 nm, 1200 nm, and 1000 nm, respectively.

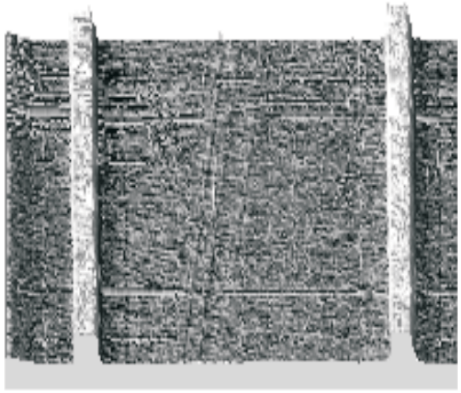

Fig. 2. Atomic force microscopy picture of the Co/CoO wire structures. The period of the parallel wire structure is equal to 15 μm.

was patterned, which is sufficient for SQUID magnetization measurements but too small for PNR experiments. Figure 1 shows scanning electron microscope (SEM) pictures of the different samples.

For the wires, with the view on the PNR experiments, UV-lithography was used and an area of 4 cm^2 was patterned. The magnetic layer is prepared by DC magnetron sputtering, followed by an in-situ oxidation by exposing the sample to pure oxygen at a pressure of 10^{-4} torr during 90 s. No buffer or cap layers were deposited. For the squares the Co thickness was approx. 22 nm, while for the wires it was 12 nm. The CoO thickness is inferred from X-ray reflectivity measurements to be 2 nm. Figure 2 shows an atomic force microscopy (AFM) picture of the wire sample surface.

The neutron reflectometer V6 of the Hahn-Meitner-Institut [23] was used for all our PNR investigations. It is a typical setup for a neutron reflectometer at a reactor source using a graphite monochromator in combination with a Be filter to produce a monochromatic neutron beam. At the V6 a wavelength $\lambda = 0.466$ nm is used. The neutron beam is collimated by two slit systems consisting of neutron absorbing diaphragms made of Cd plates. The neutrons coming from the reactor are not polarized and have a randomly distributed spin orientation. Hence, the beam needs to be polarized, which can be done very efficiently by supermirrors. They filter out one spin component by exploiting the fact that the transmission and reflection coefficients are different for spin-up and spin-down neutrons. Spin-up neutrons have their spin oriented parallel to the external field, whereas spin-down neutrons have antiparallel spin with respect to the external field. At the V6 the supermirrors consist of FeCo/Si multilayers providing an average beam polarization of 98.5 percent. The down-neutrons are transmitted and used for the experiment whereas the up-neutrons are reflected and absorbed in the diaphragm. The spin-up neutrons are produced by a Mezei-type spin flipper which rotates the neutron spin by 180 degrees by precession around a perpendicular magnetic field supplied by a coil. After the reflection at the sample surface the neutron spin can be analyzed by an additional supermirror. All four scattering cross sections, i.e. the non-spin flip (NSF) intensities I^{uu} and I^{dd} as well as the spin flip (SF) intensities I^{ud} and I^{du} can be measured. The "u" denotes up-neutrons and the "d" denotes down-neutrons. The first superscript is the spin state before the reflection, the second one after the reflection. The reflected neutrons are recorded either by ^{3}He pencil detectors or by a position sensitive detector (PSD). The PSD is a multiwire proportional counter with an active area of about 180 $\times$ 180 mm^2 and a spatial resolution of 1.5 mm. All data presented here have been corrected for inefficiencies of the optical elements.

The NSF intensities I^{uu} and I^{dd} are both generated by magnetization components (anti)parallel to the neutron spin, while the SF intensities I^{ud} and I^{du} are generated by magnetization components perpendicular to the neutron spin. For a fully magnetized sample, the intensities I^{uu} and I^{dd} differ. The spin flip intensities I^{ud} and I^{du} are always equal to each other. The ability to measure separately these four neutron cross sections provides the possibility to determine the in-plane components of the magnetization vector. This allows to discriminate between different possible magnetization reversal processes: when domain wall nucleation and motion is occurring, all magnetization vectors are either parallel or antiparallel to the applied field and NSF intensity will be recorded; in case of reversal by rotation, there will be magnetization components perpendicular to the applied field and, hence, a SF signal. PNR has been successfully used to study magnetization reversal in patterned ferromagnetic structures [24–29]. The use of the off-specular scattering geometry allows to study even small structures and relatively small sample areas.

3 Magnetization measurements

Figure 3 shows the low temperature hysteresis loops for the Co/CoO squares with size 900 nm (a), 800 nm (b),

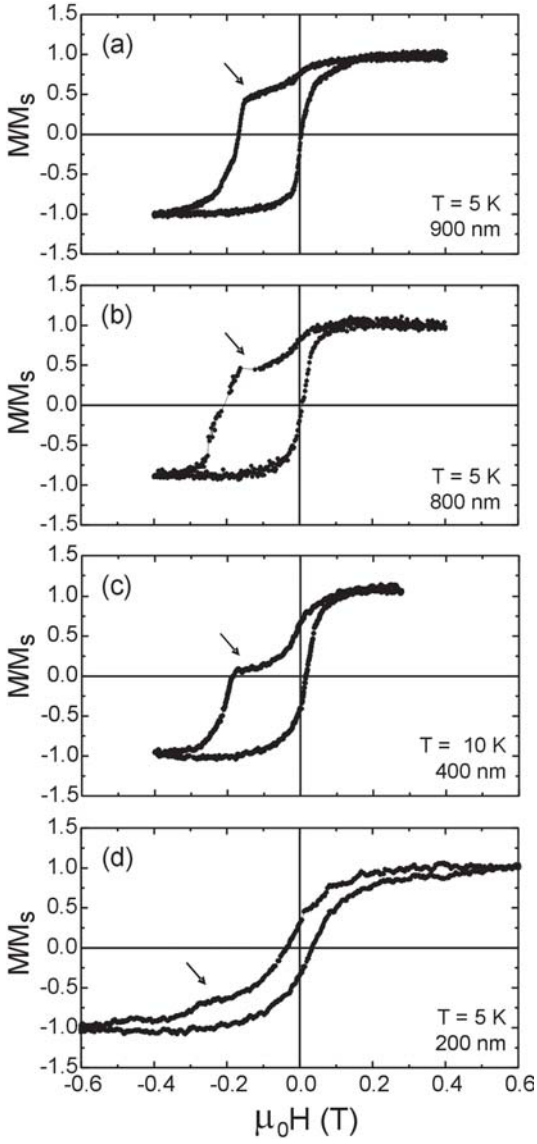

Fig. 3. Hysteresis loops of the Co/CoO square dot arrays with four different dot sizes. All magnetization curves have been measured after cooling the array in a field of 0.4 T. The arrows indicate the anomaly in the upper branch of the hysteresis loop.

400 nm (c), and 200 nm (d), respectively. The loops are measured after cooling the arrays in an in-plane magnetic field of +0.4 T, applied parallel to the side of the squares. Loop (c) was measured at a temperature of 10 K, while the other loops were measured at 5 K. Loop (b) was obtained by the SQUID, while the other loops were measured in the VSM. All loops were corrected by subtraction of the diamagnetic background caused by the substrate. The more reliable determination of zero magnetization for the SQUID measurements allows one to identify the presence of small vertical shifts of the hysteresis loops, which may be linked to the freezing of uncompensated spins.

The magnetization curves in Figure 3 reveal an asymmetry which strongly depends on the magnetic dot size: a small shoulder appears in the upper branch of the magnetization curve in Figure 3a, and this shoulder (indicated by the arrows in Fig. 3) becomes more pronounced as the size of the dots is reduced, leading to an apparent destruction of the exchange bias effect for the smallest dots in Figure 3d [13]. The presence of a partly unbiased Co layer which is free to move with the externally applied field might explain the origin of this anomaly in the upper branch of the hysteresis loop. This was inferred from minor magnetization loops, which indicate that the observed loops are a superposition of a normal ferromagnetic loop and an exchange bias-shifted loop. The relative importance of the unbiased parts increases with decreasing dimension of the Co/CoO squares and only a small fraction of biased material remains for the dots with a side of 200 nm. Since the squares are sufficiently close to each other, magnetostatic coupling between the dots may also play a role in enhancing this effect. Apart from the anomaly, it can be observed that the coercivity of the loops increases with decreasing dot size. It has been argued that this may be due to the role of the edges of the patterned structures as barriers for domain wall propagation [15].

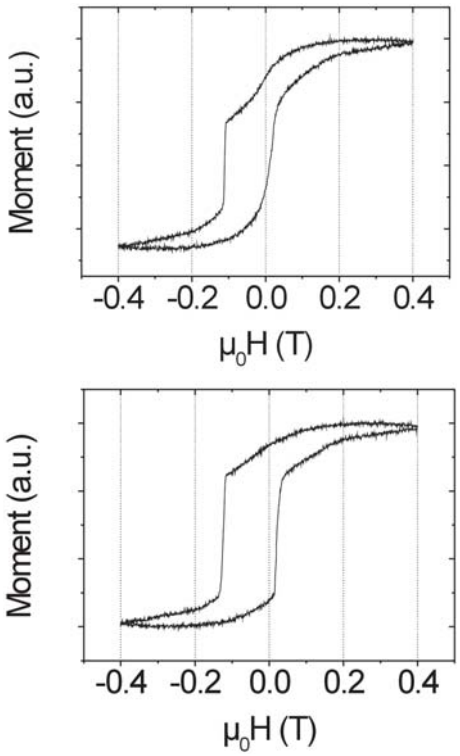

Fig. 4. Hysteresis loops of the Co/CoO wire array after cooling in a field of 0.4 T. The upper panel shows the loop with the field perpendicular to the wires; the lower panel for the field parallel to the wires.

Figure 4 shows hysteresis curves (measured using the VSM) of the Co/CoO wires at 5 K after field cooling (in a field $\mu_0 H = 0.4$ T) in fields perpendicular or parallel to the wires. The upper panel of Figure 4 shows the hysteresis curve taken with the field applied perpendicular to the wires; the lower panel shows the hysteresis curve taken with the field applied parallel to the wires. In the

perpendicular configuration the hysteresis loop clearly shows an entirely different shape compared to the parallel configuration. The hysteresis loop in the parallel configuration has a symmetrical shape, while in the perpendicular configuration the hysteresis loop shows a more asymmetric behaviour. In both configurations the exchange bias shift and the coercivity are comparable. They are also comparable to the exchange bias shift and coercivity measured in an unpatterned Co/CoO reference film. Again an anomaly can be observed in the upper branch of the hysteresis loop. The magnitude and shape of the anomaly depend on the direction of the magnetic field.

4 PNR experiments

Reference PNR measurements (not shown) on an unpatterned Co/CoO film reveal that the two branches of the hysteresis loop are characterized by different reversal mechanisms: domain wall nucleation and motion in the descending (left) branch and rotation in the ascending (right) branch, in agreement with earlier observations [20,22].

The upper panel of Figure 5 shows the spin-analyzed specular reflectivities measured at $T = 10$ K (the temperature used for all the PNR measurements on the Co/CoO wires) when the wire sample is at the first coercive field (left hand side branch of the hysteresis loop). It is subjected to a field $\mu_0 H = -0.09$ T perpendicular to the wires (after field cooling in a field of 0.4 T perpendicular to the wires). The reflectivity is obtained by normalizing the experimentally observed reflection intensity to the intensity in the total reflection regime. The non-spin-flip (down-down and up-up) reflectivities are denoted by R_{dd} and R_{uu}, respectively. The spin-flip (down-up and up-down) reflectivities are denoted by R_{du} and R_{ud}, respectively.

It can be observed that there is no magnetic splitting between the two NSF-signals. This is consistent with the absence of a net magnetization at the coercive field. The SF signal is very low and its magnitude is comparable to that measured when the sample is in the saturated state (not shown). These observations point to the presence of domain wall nucleation and motion which has set in for the magnetization reversal. It should be noted, however, that the near absence of a SF signal might also occur if the magnetic domains are much smaller than the coherence length of the neutron beam, leading to a situation where the perpendicular component of the magnetization in those domains averages out to zero and, therefore, is invisible in the SF signal. This will be investigated in the future by low-temperature domain imaging techniques.

The situation is different at the second coercive field (right hand side branch of the hysteresis loop). The lower panel of Figure 5 shows the spin-analyzed specular reflectivity at $\mu_0 H = 0.012$ T. Again there is no splitting between R_{dd} and R_{uu}, indicating the coercive state. There is now also a clear enhancement of the spin-flip intensity (the spin-flip signal lies closer to the non-spin-flip signal than at the first coercive field, see upper panel of Fig. 5),

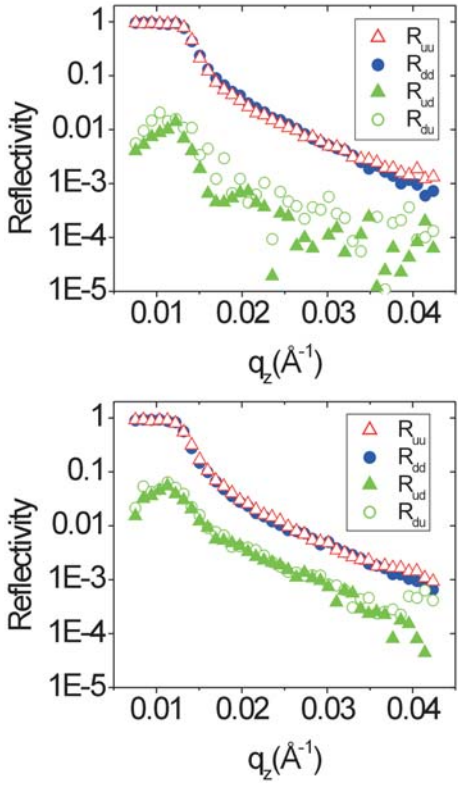

Fig. 5. NSF and SF neutron reflectivity at 10 K at the first (upper panel) and second (lower panel) coercive field of the Co/CoO wire sample for a field applied perpendicular to the wires. Prior to this experiment, the sample was cooled in a field of 0.4 T perpendicular to the wires.

pointing to the presence of a significant magnetization perpendicular to the applied field. This is consistent with a magnetization reversal occurring (mainly) by magnetization rotation. This is in agreement with the observations made on unpatterned Co/CoO films where different reversal mechanisms are active in the different branches of the hysteresis loop [20,22].

This should now be compared with the situation where the field is applied parallel to the Co/CoO wires. Prior to the measurement, the sample was cooled in a field $\mu_0 H = 0.4$ T parallel to the wires. The upper panel of Figure 6 shows the situation at the first coercive field ($\mu_0 H = -0.12$ T, applied parallel to the wires). In the coercive state there is no clear difference between the R_{dd} and R_{uu} reflectivities. The SF reflectivities are again very low and indicate that the magnetization reversal occurs by domain wall nucleation and motion.

At the second coercive field ($\mu_0 H = 0.02$ T), shown in the lower panel of Figure 6, the situation is comparable to the first coercive field, i.e., no enhancement of the SF intensity can be observed. This indicates that, for a field parallel to the lines, the magnetization reversal in both branches of the hysteresis loop occurs by domain wall nucleation and motion. The hitherto observed asymmetry in reversal mechanism is therefore suppressed in this configuration.

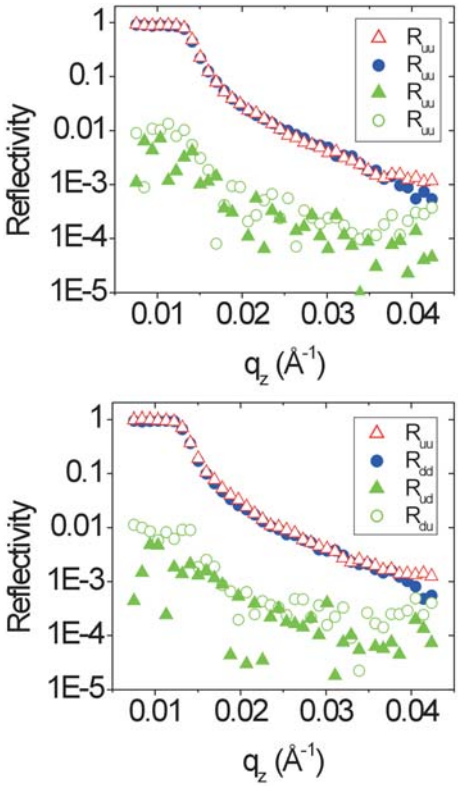

Fig. 6. NSF and SF neutron reflectivity at 10 K at the first (upper panel) and second (lower panel) coercive field of the Co/CoO wire sample for a field applied parallel to the wires. Prior to this experiment, the sample was cooled in a field of 0.4 T parallel to the wires.

5 Discussion of the PNR experiments

The PNR results suggest the following model of the magnetization reversal in a magnetic field perpendicular to the wires. At the first coercive field the reversal occurs via domain nucleation and domain wall propagation. Radu et al. [22] suggested the presence of 'interfacial domains' which are strongly coupled to the antiferromagnet and which do not get aligned with the external field direction, even in saturation. Near the interface, the magnetization in the Co layer is not free to follow the external field and, hence, a magnetization depth profile is created in the layer. These interfacial domains act as seeds for the second magnetization reversal which then occurs via domain rotation. Welp et al. [30] observed with magneto-optical imaging that during the first reversal an irregular domain pattern is created with typical domain sizes ranging between 5 μm and 10 μm. This domain structure cannot be erased, even in high fields. For a field perpendicular to the wires, the interfacial spins will align along the length of the wires, a direction favoured by the shape anisotropy. The interfacial spins will be available to seed the reversal by rotation at the second coercive field and, indeed, an enhanced spin-flip signal is observed. When the field is applied parallel to the wires, the formation of interfacial domains with spins aligned perpendicular to the long axis of the wires is not favored due to the strong shape anisotropy. In this case the interfacial domains cannot act as seeds for a second magnetization reversal by domain rotation. Instead the second magnetization reversal proceeds also via domain growth and domain wall motion, similar to the first magnetization reversal.

6 Conclusions

The influence of finite dimensions and shape anisotropy was studied in patterned Co/CoO structures. Magnetization measurements have revealed an anomaly in one branch of the low-temperature hysteresis loop, as well as a trend for increasing coercivity with decreasing feature size. Polarized neutron reflectivity was used to study the influence of shape anisotropy on the asymmetric magnetization reversal commonly observed in Co/CoO structures. For a field perpendicular to the wires the asymmetry observed in unpatterned films is retained, but for a field parallel to the wires the magnetization rotation in the ascending branch of the hysteresis loop is suppressed. This is consistent with a picture in which interfacial domains are formed during the first reversal starting from saturation: in patterned samples the shape anisotropy will favor or inhibit domain formation depending on the orientation of the applied field. Work is under way to study more systematically by PNR structures with different sizes and aspect ratios, as well as the behavior of the asymmetry when the measurement field is applied under an angle with respect to the cooling field direction, as was recently discussed theoretically [31].

This work was supported by the Fund for Scientific Research - Flanders (FWO), the Flemish GOA and Belgian IAP Programs, the Flanders-Chile Bilateral Agreement (BIL00/01), and by the European Commission under the Human Potential Program (HPRI-1999-CT00020) and the QMDS Research and Training Network (HPRN-CT-2000-00134). K.T. and M.J.V.B. are Post-Doctoral Research Fellow of the FWO. The authors wish to thank F. Radu, H. Zabel, and I.K. Schuller for stimulating discussions.

References

1. M. Hehn, K. Ounadjela, J.P. Bucher, F. Rousseaux, D. Decanini, B. Bartenlian, C. Chappert, Science **272**, 1782 (1996)
2. C.A. Ross, S. Haratani, F.J. Castaño, Y. Hao, M. Hwang, M. Shima, J.Y. Cheng, B. Vögeli, M. Farhoud, M. Walsh, H.I. Smith, J. Appl. Phys. **91**, 6848 (2002)
3. L.C. Sampaio, R. Hyndman, F.S. de Menezes, J.P. Jamet, P. Meyer, J. Gierak, C. Chappert, V. Mathet, J. Ferré, Phys. Rev. B **64**, 4440 (2001)
4. P.D. Ye, D. Weiss, R.R. Gerhardt, H. Nickel, J. Appl. Phys. **81**, 5444 (1997)
5. J.I. Martín, M. Vélez, A. Hoffmann, I.K. Schuller, J.L. Vicent, Phys. Rev. Lett. **83**, 1022 (1999)
6. M.J. Van Bael, K. Temst, V.V. Moshchalkov, Y. Bruynseraede, Phys. Rev. B **59**, 14674 (1999)

7. For a review of experimental work on exchange bias, see J. Nogués, I.K. Schuller, J. Magn. Magn. Mater. **192**, 203 (1999)
8. For a review of theoretical work on exchange bias, see M. Kiwi, J. Magn. Magn. Mater. **243**, 584 (2001)
9. M. Fraune, U. Rüdiger, G. Güntherodt, S. Cardoso, P. Freitas, Appl. Phys. Lett. **77**, 3815 (2000)
10. K. Liu, S.M. Bader, M. Tuominen, T.P. Russell, I.K. Schuller, Phys. Rev. B **63**, 060403 (2001)
11. S. Zhang, Z. Li, Phys. Rev. B **65**, 054406 (2001)
12. T. Pokhil, D. Song, E. Linville, J. Appl. Phys. **91**, 6887 (2002)
13. E. Girgis, R.D. Portugal, H. Loosvelt, M.J. Van Bael, I. Gordon, M. Malfait, K. Temst, C. Van Haesendonck, L.H.A. Leunissen, R. Jonckheere, Phys. Rev. Lett. **91**, 187202 (2003)
14. A. Hoffmann, M. Grimsditch, J.E. Pearson, J. Nogués, W.A. Macedo, I.K. Schuller, Phys. Rev. B **67**, 220406 (2003)
15. J. Sort, B. Diény, M. Fraune, C. Koenig, F. Lunnebach, B. Beschoten, G. Güntherodt, Appl. Phys. Lett. **84**, 3696 (2004)
16. V. Baltz, J. Sort, B. Rodmacq, B. Diény, S. Landis, Appl. Phys. Lett. **84**, 4923 (2004)
17. H. Zabel, K. Theis-Bröhl, J. Phys.: Condens. Mater. **15**, S505 (2003)
18. M.R. Fitzsimmons, S.D. Bader, J.A. Borchers, G.P. Felcher, J.K. Furdyna, A. Hoffmann, J.B. Kortright, I.K. Schuller, T.C. Schulthess, S.K. Sinha, M.F. Toney, D. Weller, S. Wolf, J. Magn. Magn. Mater. **271**, 103 (2004)
19. M.R. Fitzsimmons, P. Yashar, C. Leighton, I.K. Schuller, J. Nogués, C.F. Majkrzak, J.A. Dura, Phys. Rev. Lett. **84**, 3986 (2000)
20. M. Gierlings, M.J. Prandolini, H. Fritzsche, M. Gruyters, D. Riegel, Phys. Rev. B **65**, 92407 (2002)
21. W.-T. Lee, S.G.E. te Velthuis, G.P. Felcher, F. Klose, T. Gredig, E.D. Dahlberg, Phys. Rev. B **65**, 224417 (2002)
22. F. Radu, M. Etzkorn, R. Siebrecht, T. Schmitte, K. Westerholt, H. Zabel, Phys. Rev. B **67**, 134409 (2003)
23. F. Mezei, R. Golub, F. Klose, H. Toews, Physica B **213-214**, 898 (1995)
24. K. Temst, M.J. Van Bael, H. Fritzsche, Appl. Phys. Lett. **79**, 991 (2001)
25. N.D. Telling, S. Langridge, R.M. Dalgliesh, P.J. Grundy, V.M. Vishnyakov, J. Appl. Phys. **93**, 7420 (2003)
26. K. Theis-Bröhl, T. Schmitte, V. Leiner, H. Zabel, K. Rott, H. Brückl, J. McCord, Phys. Rev. B **67**, 184415 (2003)
27. H. Fritzsche, M.J. Van Bael, K. Temst, Langmuir **19**, 7789 (2003)
28. H. Fritzsche, K. Temst, M.J. Van Bael, Recent Res. Devel. Applied Phys. **6**, 105 (2003)
29. K. Temst, M.J. Van Bael, J. Swerts, H. Loosvelt, E. Popova, D. Buntinx, J. Bekaert, C. Van Haesendonck, Y. Bruynseraede, R. Jonckheere, H. Fritzsche, Superlattices and Microstructures **34**, 87 (2003)
30. U. Welp, S.G.E. te Velthuis, G.P. Felcher, T. Gredig, E.D. Dahlberg, J. Appl. Phys. **93**, 7726 (2003)
31. B. Beckmann, U. Nowak, K.D. Usadel, Phys. Rev. Lett. **91**, 187201 (2003)